Cooperative regulation of $Ca_v1.2$ channels by intracellular Mg^{2+}, the proximal C-terminal EF-hand, and the distal C-terminal domain

Sylvain Brunet, Todd Scheuer, and William A. Catterall

Department of Pharmacology, University of Washington, Seattle, WA 98195

L-type Ca^{2+} currents conducted by $Ca_v1.2$ channels initiate excitation–contraction coupling in cardiac myocytes. Intracellular Mg^{2+} (Mg_i) inhibits the ionic current of $Ca_v1.2$ channels. Because Mg_i is altered in ischemia and heart failure, its regulation of $Ca_v1.2$ channels is important in understanding cardiac pathophysiology. Here, we studied the effects of Mg_i on voltage-dependent inactivation (VDI) of $Ca_v1.2$ channels using Na^+ as permeant ion to eliminate the effects of permeant divalent cations that engage the Ca^{2+}-dependent inactivation process. We confirmed that increased Mg_i reduces peak ionic currents and increases VDI of $Ca_v1.2$ channels in ventricular myocytes and in transfected cells when measured with Na^+ as permeant ion. The increased rate and extent of VDI caused by increased Mg_i were substantially reduced by mutations of a cation-binding residue in the proximal C-terminal EF-hand, consistent with the conclusion that both reduction of peak currents and enhancement of VDI result from the binding of Mg_i to the EF-hand ($K_D \approx 0.9$ mM) near the resting level of Mg_i in ventricular myocytes. VDI was more rapid for L-type Ca^{2+} currents in ventricular myocytes than for $Ca_v1.2$ channels in transfected cells. Coexpression of $Ca_v\beta_{2b}$ subunits and formation of an autoinhibitory complex of truncated $Ca_v1.2$ channels with noncovalently bound distal C-terminal domain (DCT) both increased VDI in transfected cells, indicating that the subunit structure of the $Ca_v1.2$ channel greatly influences its VDI. The effects of noncovalently bound DCT on peak current amplitude and VDI required Mg_i binding to the proximal C-terminal EF-hand and were prevented by mutations of a key divalent cation-binding amino acid residue. Our results demonstrate cooperative regulation of peak current amplitude and VDI of $Ca_v1.2$ channels by Mg_i, the proximal C-terminal EF-hand, and the DCT, and suggest that conformational changes that regulate VDI are propagated from the DCT through the proximal C-terminal EF-hand to the channel-gating mechanism.

INTRODUCTION

Intracellular Mg^{2+} (Mg_i) is not used as a signaling molecule in normal cellular function, and its concentration is thought to be nearly constant under physiological conditions. However, Mg_i increases after transient ischemia in the heart (Murphy et al., 1989; Headrick and Willis, 1991) and decreases in heart failure (Haigney et al., 1998). Altered Mg_i is also observed in pathophysiological conditions in the brain (Resnick et al., 2004; Mendez et al., 2005) and skeletal muscle (Resnick et al., 2004). Elucidation of the regulatory effects of Mg_i under these pathophysiological conditions would be an important advance toward understanding the impairments of cell function in these disease states.

L-type Ca^{2+} currents initiate excitation–contraction coupling in cardiac muscle cells (Reuter, 1979; Bers, 2002). Mg_i inhibits the L-type Ca^{2+} currents in ventricular myocytes at physiologically relevant concentrations in the range of 0.8 mM (White and Hartzell, 1988; Agus et al., 1989; Yamaoka and Seyama, 1996a; Pelzer et al., 2001; Wang et al., 2004). L-type Ca^{2+} currents in ventricular myocytes are conducted by $Ca_V1.2$ channels consisting of a pore-forming $\alpha_1 1.2$ subunit in association with β and $\alpha_2\delta$ subunits (Catterall, 2000). The α_1 subunits are composed of four homologous domains (I–IV) with six transmembrane segments (S1–S6) and a reentrant pore loop in each. Multiple regulatory sites are located in the large C-terminal domain (De Jongh et al., 1996; Peterson et al., 1999; Zuhlke et al., 1999; Hulme et al., 2003), which is subject to in vivo proteolytic processing near its center (De Jongh et al., 1991, 1996; Hulme et al., 2005). A nearby IQ motif in the proximal C terminus is implicated in Ca^{2+}-dependent inactivation mediated by Ca^{2+}/calmodulin (Peterson et al., 1999; Zuhlke et al., 1999). Noncovalent interaction of the distal C terminus with the proximal C-terminal domain has an autoinhibitory effect by reducing coupling efficiency of gating charge movement to channel opening and positively shifting the voltage dependence of activation (Hulme et al., 2006). The proximal C-terminal domain also contains an EF-hand motif, a potential divalent

Correspondence to Sylvain Brunet: sbrunet@u.washington.edu

Abbreviations used in this paper: DCRD, distal C-terminal regulatory domain; HP, holding potential; Mg_i, intracellular Mg^{2+}; PCRD, proximal C-terminal regulatory domain; VDI, voltage-dependent inactivation; WT, wild-type.

The Rockefeller University Press $30.00
J. Gen. Physiol. Vol. 134 No. 2 81–94
www.jgp.org/cgi/doi/10.1085/jgp.200910209

cation-binding site and a prime candidate for mediating inhibition by Mg_i.

Upon maintained depolarization, L-type calcium currents in neurons, cardiac myocytes, and other cell types inactivate by a dual mechanism dependent on both Ca^{2+} and voltage (Brehm and Eckert, 1978; Tillotson, 1979; Ashcroft and Stanfield, 1981; Lee et al., 1985; Nilius and Benndorf, 1986). Inactivation plays an important role in the control of the action potential duration and excitation–contraction coupling (Kleiman and Houser, 1988; Keung, 1989; Ahmmed et al., 2000). The physiological significance of voltage-dependent inactivation (VDI) is illustrated by the dramatic effects of missense mutations that impair VDI in Timothy syndrome (Splawski et al., 2004), which is characterized by prolonged QT interval, prolonged action potential duration, and severe ventricular arrhythmias in the heart, as well as by developmental abnormalities in other tissues and autism spectrum disorder in the brain (Splawski et al., 2004, 2005).

Our previous work showed that Mg_i inhibits $Ca_V1.2$ channels in transfected cells in the same concentration range as in cardiac myocytes, and implicated the proximal C-terminal EF-hand motif in the reduction of peak L-type Ca^{2+} currents of $Ca_V1.2$ channels by Mg_i (Brunet et al., 2005a,b). In the experiments described here, we have examined whether the autoinhibitory action of the distal C-terminal domain interacts functionally with the inhibition of $Ca_V1.2$ channel activity by the binding of Mg_i to the EF-hand. Using Na^+ as permeant ion to eliminate effects of permeant divalent cations, we confirm that Mg_i reduces the amplitude and increases VDI of L-type Ca^{2+} currents in ventricular myocytes. With these recording methods, we find that Mg_i also increases VDI of transfected $Ca_V1.2$ channels through interaction with the proximal C-terminal EF-hand. In addition, we show that an autoinhibitory complex containing the distal C-terminal domain noncovalently bound to the proximal C-terminal domain greatly enhances VDI of $Ca_V1.2$ channels in transfected tsA-201 cells. The binding of Mg_i to the proximal C-terminal EF-hand is required for the distal C-terminal domain to exert its autoinhibitory effects. Our results indicate that the EF-hand with bound Mg^{2+} is required for inhibition of $Ca_V1.2$ channel activity by the distal C-terminal domain, and suggest cooperative regulation of channel function by the distal C-terminal domain and Mg_i binding to the proximal C-terminal EF-hand.

MATERIALS AND METHODS

Ventricular myocyte isolation

Left ventricular myocytes were isolated from 8–12-wk-old female adult C57/BL6 mice as described previously (Brunet et al., 2004) and maintained at 37°C until use. All protocols were approved by the University of Washington Institutional Animal Care and Use Committee.

cDNA constructs

The C-terminal truncation of $\alpha_1$1.2a Δ1821 and Δ1800 were generated by introducing a stop codon after amino acid residues 1,821 and 1,800, respectively, using cDNA encoding the rabbit $\alpha_1$1.2a (Mikami et al., 1989) as template. $Ca_V1.2$ EF-hand single (D1546A/N/S/R/K) and double (E1537Q, D1546N) mutants; the mutant $\alpha_1$1.2aΔ1800(D1546R); and the triple mutant $distal_{1822–2171}$(E2103Q,E2106Q,D2110Q), abbreviated EED-QQQ, were constructed using PCR overlap extension (Brunet et al., 2005b; Hulme et al., 2006). The mutant sequence, orientation, and reading frame of all constructs were confirmed by DNA sequencing.

Cell culture

TsA-201 cells were grown to 80% confluence and transfected with an equimolar ratio of cDNA encoding full-length, truncated, or mutant α1.2a, $Ca_V\beta$ ($Ca_V\beta_{1b}$, $Ca_V\beta_{2a}$, or $Ca_V\beta_{2b}$), $Ca_V\alpha_2\delta_1$, and CD8 as a cell surface marker (EBO-pCD-Leu2; American Type Culture Collection) using Fugene (Roche). 15–24 h after transfection, cells were suspended, plated at low density in 35-mm dishes, and incubated at 37°C in 10% CO_2 for at least 17 h before recording using the whole cell configuration of the patch clamp technique. Transiently transected cells were visualized with latex beads conjugated to an anti-CD8 antibody (Invitrogen).

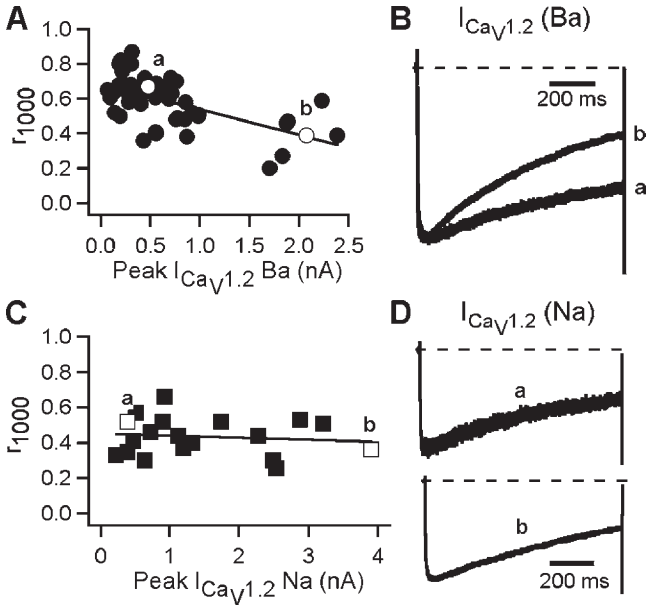

Figure 1. Effects of Ba^{2+} and Na^+ ion as charge carrier on VDI of $Ca_V1.2$ current expressed in tsA-201 cells. (A) Relationship between r_{1000} and current amplitude of $Ca_V1.2$ currents (n = 52) with Ba as charge carrier $I_{CaV1.2}$(Ba). The straight line represents a linear regression (r = −0.61; P < 0.001). (B) Inactivation of typical current traces from cells with low and high current amplitudes (cells a and b from A). (C) Relationship between r_{1000} and current amplitude of $Ca_V1.2$ currents (n = 19) with Na^+ as charge carrier $I_{CaV1.2}$(Na). The straight line represents a linear regression (r = −0.11; P = NS). (D) Inactivation of typical current traces from cells with low and high current amplitudes (cells a and b from C). Currents were elicited by a depolarization to 0 mV for 1,000 ms from a HP of −80 mV and normalized to their peak amplitudes. The Mg_i concentration was 0.8 mM. Dotted lines in this and all figures represent the zero current level.

Electrophysiology

Patch pipettes (2.5–3.5 MΩ) were pulled from micropipette glass (VWR Scientific) and fire-polished. Currents were recorded with an Axopatch 200B amplifier (MDS Analytical Technologies) and sampled at 5 kHz after anti-alias filtering at 2 kHz. Data acquisition and command potentials were controlled by Pulse (Pulse 8.50; HEKA), and data were stored for off-line analysis. Voltage protocols were delivered at 10-s intervals unless otherwise noted, and leak and capacitive transients were subtracted using a P/4 protocol. Approximately 80% of series resistance was compensated with the voltage clamp circuitry.

For whole cell voltage clamp recordings of $Ca_V1.2$ current in tsA-201 cells with Ba^{2+} as a charge carrier ($I_{CaV1.2}(Ba)$), the extracellular bath solution contained (in mM): 10 $BaCl_2$, 140 Tris, 2 $MgCl_2$, and 10 D-glucose, titrated to pH 7.3 with $MeSO_4$. The normal intracellular Mg (0.8 mM free Mg_i) solution contained (in mM): 130 *N*-methyl-D-glucamine, 60 HEPES, 5 MgATP, 1 $MgCl_2$, and 10 EGTA, titrated to pH 7.4 with $MeSO_4$. For coupling ratio determination, the intracellular solution contained (in mM): 130 CsCl, 10 HEPES, 4 MgATP, 1 $MgCl_2$, and 10 EGTA titrated to pH 7.3 with CsOH (Hulme et al., 2006). When Na^+ was used as charge carrier ($I_{CaV1.2}(Na)$), the extracellular solution contained (in mM): 150 NaCl, 10 HEPES, 0.2 $MgCl_2$, 0.25 μM EDTA, and 10 D-glucose titrated to pH 7.3 with $MeSO_4$. The normal intracellular Mg (0.8 mM free Mg) solution contained (in mM): 150 CsOH, 110 glutamate, 20 HCl, 10 HEPES, 5 MgATP, 1 $MgCl_2$, and 10 EGTA titrated to pH 7.6 with CsOH (Ferreira et al., 1997).

For whole cell voltage clamp recordings of ventricular myocyte L-type Ca^{2+} currents with Ca^{2+} as charge carrier ($I_{Ca,L}(Ca)$), the extracellular solution contained (in mM): 1.8 $CaCl_2$, 140 TEA-Cl, 2 $MgCl_2$, 10 D-glucose, and 10 HEPES, pH 7.3 with CsOH. The normal Mg intracellular solution (0.8 mM Mg_i) contained (in mM): 100 CsCl, 20 TEA-Cl, 10 EGTA, 10 HEPES, 5 MgATP, and 1 $MgCl_2$ titrated to pH 7.3 with CsOH. When Na^+ was the charge carrier $I_{Ca,L}(Na)$, the extracellular recording solution contained (in mM): 100 NaCl, 40 TEA-Cl, 0.7 $MgCl_2$, 5 CsCl, 10 HEPES, 10 D-glucose, and 0.250 μM EDTA, pH 7.3 with CsOH. The intracellular solution (0.8 mM Mg_i) contained (in mM): 110 CsOH, 40 TEA-Cl, 110 glutamate, 20 HCl, 1 $MgCl_2$, 10 HEPES, 5 MgATP, and 10 EGTA titrated to pH 7.6 with CsOH (Ferreira et al., 1997). The Mg_i concentration was altered by changing the amount of $MgCl_2$ added to the intracellular solution. Free Mg_i was calculated by the MaxChelator program (Bers, 2002).

Data analysis

Voltage clamp data were compiled and analyzed using IGOR Pro (WaveMetrics Inc.) and Excel (Microsoft). Peak currents were measured during 300-ms (for L-type Ca^{2+} current) or 1,000-ms (for $Ca_V1.2$ current) depolarization to potentials between −50 and 70 mV for L-type Ca^{2+} currents, and −80 to 20 mV for $Ca_V1.2$ currents. To quantify inactivation, peak currents elicited by 300- or 1,000-ms depolarizations to 0 mV were normalized to 1.0, and the fraction of peak current remaining at the end of the voltage pulse (r_{300} or r_{1000}) was measured. For steady-state inactivation parameters, tsA-201 cells were depolarized from a holding potential (HP) of −80 mV for 4 s to membrane potentials from −80 to 20 mV in 10-mV increments. Na^+ currents were then elicited by a 30-ms depolarization to 30 mV, followed by repolarization to −40 mV to measure tail currents. Pulses were applied every 30 s. L-type Ca^{2+} current density (pA/pF) was defined as the peak current elicited by the voltage depolarization normalized to the whole cell membrane capacitance (within the same myocyte).

All data are presented as mean ± SEM. The statistical significance of differences between the various experimental groups was evaluated using the Student's *t* test or one-way ANOVA, followed by the Newman-Keuls post-test; p-values are presented in the text.

RESULTS

VDI of $Ca_V1.2$ channels

In our previous studies, we found that increased Mg_i reduces peak Ba^{2+} currents conducted by $Ca_V1.2$ channels expressed in tsA-201 cells (Brunet et al., 2005b). To determine whether Mg_i modulates VDI of cloned $Ca_V1.2$ channels, we initially examined the effect of Mg_i on the inactivation properties of $Ca_V1.2$ channels

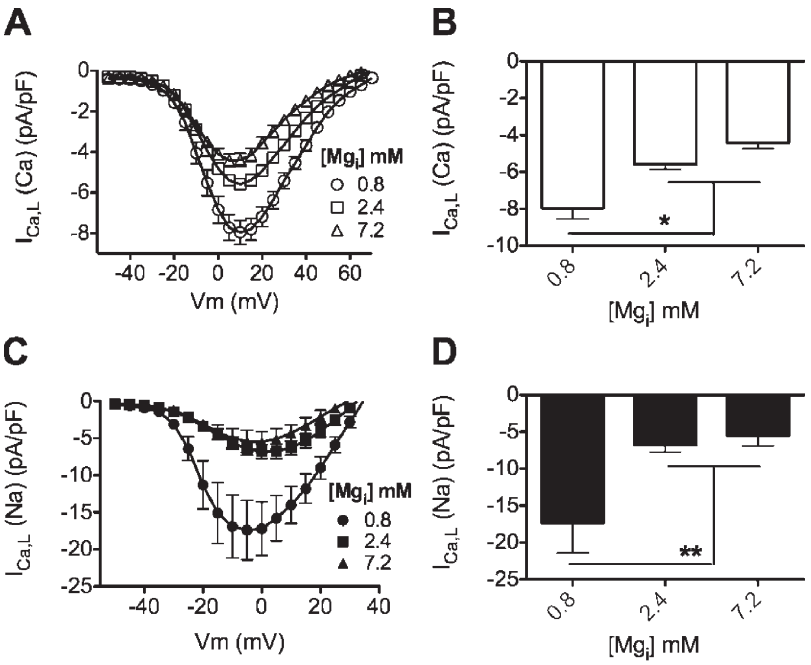

Figure 2. Mg_i dependence of L-type Ca^{2+} current density in mouse ventricular myocytes with Ca^{2+} and Na^+ as charge carriers. (A) Effect of Mg_i on $I_{Ca,L}(Ca)$ density. Currents were elicited by 300-ms depolarizations from an HP of −50 mV to the indicated potentials from −50 to 70 mV. (B) Mean peak $I_{Ca,L}(Ca)$ density with different Mg_i concentrations. n = 13, 8, and 11 myocytes for 0.8, 2.4, and 7.2 mM Mg_i, respectively. (C) Effect of Mg_i on $I_{Ca,L}(Na)$ density. (D) Mean peak $I_{Ca,L}(Na)$ density measured at different Mg_i concentrations. n = 7, 6, and 6 myocytes for 0.8, 2.4, and 7.2 mM Mg_i, respectively. Error bars are ± SEM in this and all subsequent figures. In this and all figures, * and ** indicate $P < 0.05$ and $P < 0.01$, respectively.

expressed in tsA-201 cells using Ba^{2+} as the charge carrier. This approach reduces Ca^{2+}-dependent inactivation because Ba^{2+} does not bind with high affinity to calmodulin, which mediates Ca^{2+}-dependent inactivation by binding to an IQ motif in the C-terminal domain (Peterson et al., 1999; Zuhlke et al., 1999). Ba^{2+} currents inactivated slowly as expected (Fig. 1, A and B). However, the rate of inactivation depended on the size of the Ba^{2+} current (Fig. 1, A and B). Using the ratio of inward current at the end of a 1,000-ms test depolarization to the peak current (r_{1000}) as an index of inactivation, we found a significant increase in inactivation with larger peak Ba^{2+} current amplitude ($r = -0.61$; $P < 0.001$) (Fig. 1, A and B). Because of this Ba^{2+}-dependent effect on inactivation, we could not use Ba^{2+} as a charge carrier to examine the effect(s) of Mg_i on VDI of $Ca_V1.2$ channels unambiguously. To avoid such effects of permeant divalent cations, we used Na^+ as charge carrier to measure VDI independently of divalent cation–dependent inactivation.

When extracellular Ca^{2+} is reduced below micromolar level, $Ca_V1.1$ and $Ca_V1.2$ channels become permeable to monovalent cations (Almers et al., 1984; Hess and Tsien, 1984; Hadley and Hume, 1987), allowing measurements of $Ca_V1.2$ channel activity in the absence of permeant divalent cations. As anticipated, no correlation between the peak current amplitude and r_{1000} was observed with Na^+ as charge carrier ($r = -0.11$; P = NS) (Fig. 1, C and D). These results show that large Ba^{2+} currents induce cation-dependent inactivation, presumably caused by low affinity binding of Ba^{2+} to calmodulin. Similar effects of Ba^{2+} have been observed previously (Ferreira et al., 1997; Sun et al., 2000). Except where indicated, Na^+ was used as charge carrier to examine the effects of Mg_i on VDI of $Ca_V1.2$ channels in our subsequent experiments.

Reduction of peak L-type Ca^{2+} currents in ventricular myocytes by Mg_i

Mg_i inhibits L-type Ca^{2+} currents of cardiac myocytes (White and Hartzell, 1988; Yamaoka and Seyama, 1996a; Wang et al., 2004). As a baseline for our experiments, we examined the impact of changing Mg_i on the L-type Ca^{2+} currents of mouse ventricular myocytes (Fig. 2). With Ca^{2+} as a charge carrier, increasing Mg_i from the normal resting value of 0.8 to 2.4 mM, a pathophysiologically relevant concentration (Murphy et al., 1989), decreased mean $I_{Ca,L}(Ca)$ density from -8.0 ± 0.6 pA/pf ($n = 13$) to -5.6 ± 0.3 pA/pf ($n = 8$; $P < 0.05$) (Fig. 2, A and B). Further reduction was observed with 7.2 mM Mg_i (Fig. 2, A and B). The reduction in current density when Mg_i was increased from 0.8 to 2.4 mM was greater with Na^+ as charge carrier ($61 \pm 5\%$; $n = 6$) compared with Ca^{2+} as charge carrier ($30 \pm 3\%$; $P < 0.001$), and an additional decrease was observed at 7.2 mM Mg_i (Fig. 2, C and D).

Enhancement of VDI of L-type Ca^{2+} currents of ventricular myocytes by Mg_i

In ventricular myocytes, the rate of inactivation of $I_{Ca,L}$ (Na) currents was reduced compared with $I_{Ca,L}(Ca)$ currents, as observed previously (Sun et al., 2000) (Fig. 3 A). The value of r_{300} for $I_{Ca,L}(Na)$ decreased from 0.44 ± 0.02 ($n = 9$) with 0.8 mM Mg_i to 0.30 ± 0.02 ($n = 13$) with 2.4 mM Mg_i ($P < 0.01$), and 7.2 mM Mg_i caused a further reduction (Fig. 3, B and C). The reduction of peak $Ca_V1.2$ current (Fig. 2) plus the acceleration of VDI (Fig. 3) would work together to markedly reduce Ca^{2+} entry when Mg_i is elevated in cardiac myocytes.

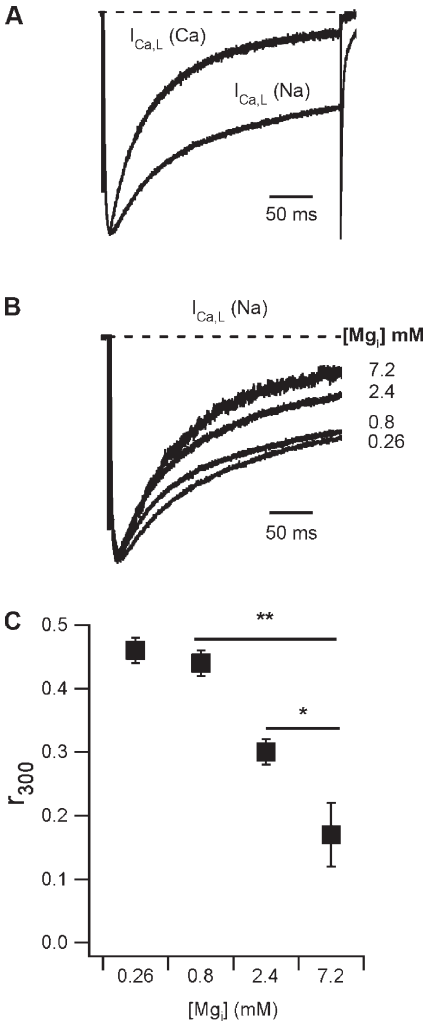

Figure 3. Mg_i modulation of VDI of L-type calcium current from mouse ventricular myocytes. (A) Comparison of VDI with Ca^{2+} versus Na^+ as charge carrier. Normalized and averaged current traces for Ca^{2+} $I_{Ca,L}(Ca)$ ($n = 6$) and Na^+ $I_{Ca,L}(Na)$ ($n = 9$). (B) Effect of Mg_i on the inactivation of $I_{Ca,L}(Na)$. Normalized average current traces are shown. (C) Plot of r_{300} versus Mg_i concentrations. $n = 4$, 9, 13, and 10 for 0.26, 0.8, 2.4, and 7.2 mM Mg_i, respectively.

Effects of Mg_i on VDI of $Ca_V1.2$ channels in tsA-201 cells

To determine whether Mg_i modulates VDI of $Ca_V1.2$ channels expressed in tsA-201 cells, we measured $I_{Ca,L}(Na)$ with a range of Mg_i concentrations (0.26–7.2 mM). Increased Mg_i enhanced the rate and extent of VDI of $Ca_V1.2$ current (Fig. 4 A), with an apparent K_d of 0.9 mM (Fig. 4 B). Coexpression of the calmodulin mutant CaM_{1234}, in which mutations of all four EF-hands prevent Ca^{2+} binding and Ca-dependent inactivation (Peterson et al., 1999), had no effect on the measured inactivation (Fig. 4 C). These results indicate that only VDI is observed under our recording conditions.

Effects of EF-hand mutations on VDI

To determine the role of the C-terminal EF-hand in modulating VDI, we tested the EF-hand mutations D1546A/N/S/K/R, which reduce the effects of Mg_i on peak Ba^{2+} currents compared with wild-type (WT) $Ca_V1.2$ channels (Brunet et al., 2005b). These mutations significantly reduced VDI, as assessed from the ratio of r_{1000} values at 0.26 and 2.4 mM Mg_i (Fig. 4 D). The rank order of effects (K>R>S>N>A) was the same as previously observed for reduction of peak currents by Mg_i (Brunet et al., 2005b), consistent with the conclusion that Mg^{2+} binds to the proximal C-terminal EF-hand and causes both effects.

To further explore the role of Mg_i and the EF-hand in modulation of VDI, we studied steady-state inactivation of WT $Ca_V1.2$ or EF-hand mutant (D1546K) channels expressed in tsA-201 cells. For WT $Ca_V1.2$ channels at low Mg_i concentration, steady-state inactivation was incomplete compared with higher Mg_i concentrations (Fig. 5 A and Table I). Elevation of Mg_i resulted in a negative shift in the voltage dependence of inactivation and an increase of maximal inactivation at positive potentials (Fig. 5 A). These effects are similar to those observed when Ba^{2+} was used as charge carrier for transfected $Ca_V1.2$ channels (Brunet et al., 2005b) and for myocyte L-type Ca^{2+} currents (Hartzell and White, 1989). Complete inactivation at depolarized potentials was observed with 2.4 and 7.2 mM Mg_i in these experiments using Na^+ as a charge carrier (Fig. 5 A and Table I), but not when Ba^{2+} was the permeant ion (Brunet et al., 2005b).

To test the role of the proximal C-terminal EF-hand in the enhancement of steady-state inactivation by Mg_i, we examined the effects of Mg_i on the mutant D1546K. Mg_i caused a similar negative shift of the voltage dependence of inactivation for this mutant compared with WT, suggesting that the negative shift of the voltage dependence of inactivation does not require binding to the EF-hand. However, steady-state inactivation of mutant D1546K was less complete at the most positive prepulse potential (+20 mV) than WT at each concentration of Mg_i (Fig. 5 B and Table I, $I_{non\text{-}inact}$). When plotted as a concentration–response curve, the dependence of the extent of inactivation at +20 mV on Mg_i is shifted to higher concentrations by the mutation D1546K with a half-maximal effect at 0.78 ± 0.04 mM Mg_i in WT compared with 3.6 ± 1.4 mM Mg_i for the mutant, a ratio of 4.6 ± 0.39 (Fig. 5 C). This decrease in apparent affinity for Mg_i in enhancing the extent of VDI caused by the mutation D1546K is similar to the decrease of 3.6-fold in the apparent affinity for Mg_i in increasing the rate of VDI that is caused by the same mutation (Fig. 4 D). These results are consistent with the conclusion that both the effect of the mutation on the rate of VDI and the effect on the extent of VDI arise from the same mechanism-impaired affinity for Mg_i binding to the proximal C-terminal EF-hand.

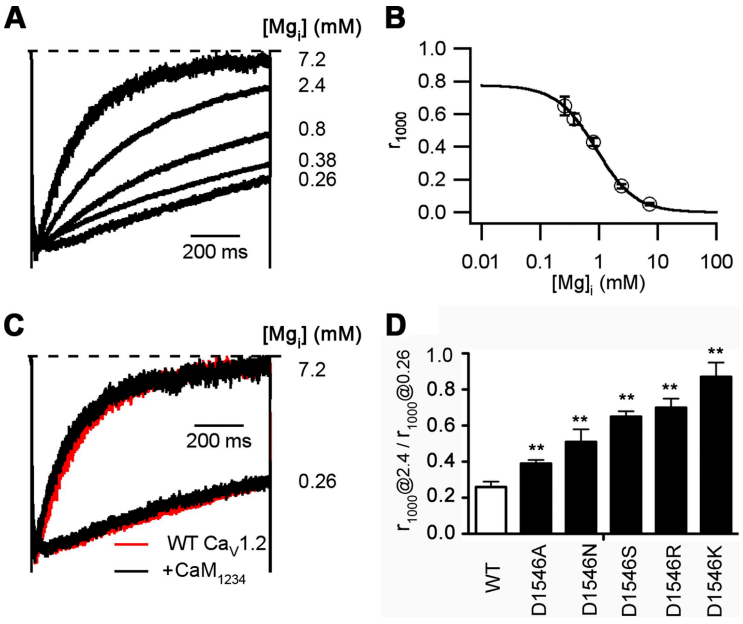

Figure 4. Effect of Mg_i on VDI of WT $Ca_V1.2$ and C-terminal EF-hand mutant channels expressed in tsA-201 cells using Na^+ as charge carrier. Currents were elicited by 1,000-ms steps to 0 mV from an HP of −80 mV. (A) Dependence of VDI of $Ca_V1.2(Na)$ current on Mg_i. n = 8, 12, 19, 15, and 15 for 0.26 0.38, 0.8, 2.4, and 7.2 mM Mg_i, respectively. (B) Plot of r_{1000} versus log[Mg_i]. Curve represents the best fit of a binding isotherm to the data. The apparent K_d was 0.9 ± 0.1 mM. (C) Effects of Mg_i on VDI of $Ca_V1.2$ with the coexpression of CaM_{1234}. A calmodulin (CaM) construct containing alanine substitutions for critical aspartate residues that impair Ca^{2+} coordination in the paired EF-hand of both lobes of CaM (CaM_{1234}) was expressed in molar excess relative to the Ca^{2+} channel subunits. n = 3 and 4 for 0.26 and 7.2 mM Mg_i, respectively. (D) Dependence of VDI of C-terminal EF-hand mutant of $Ca_V1.2$ on Mg_i. Mean ratio of r_{1000} with 2.4 mM Mg_i to r_{1000} with 0.26 mM Mg_i (r_{1000} at 2.4 mM/r_{1000} at 0.26 mM) for each $Ca_V1.2$ C-terminal EF-hand mutant. Number of cells at 0.26 and 2.4 mM Mg_i were WT: 9 and 11; D1546A: 7 and 9; D1546N: 6 and 4; D1546S: 6 and 4; D1546R: 5 and 7; and D1546K: 4 and 6.

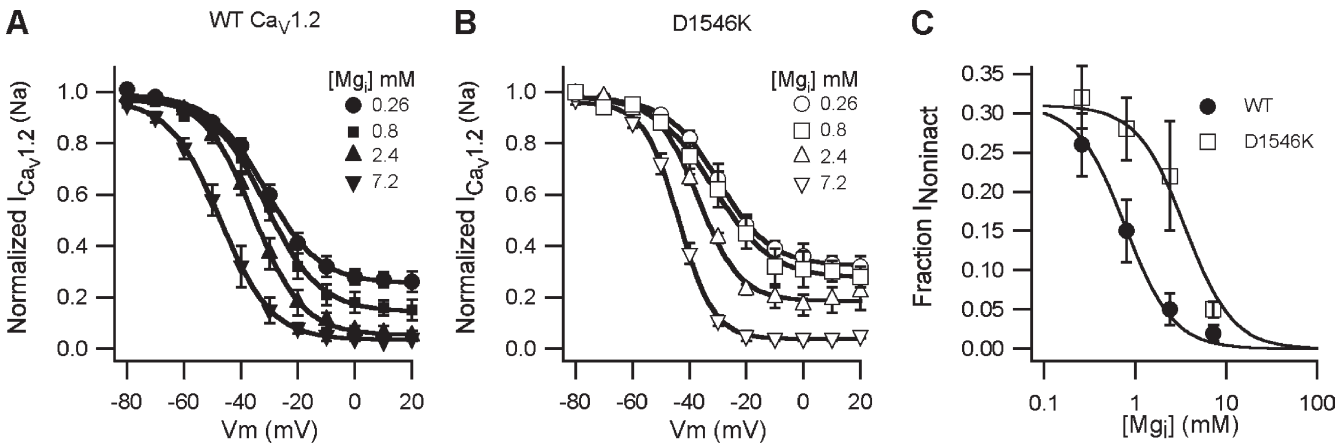

Figure 5. Mg_i modulation of the voltage dependence of inactivation of WT $Ca_V1.2$ and C-terminal EF-hand mutant ($Ca_V1.2$(D1546K)) with Na^+ as charge carrier. Comparison of mean inactivation–voltage relationships for $I_{CaV1.2}$(Na) of WT $Ca_V1.2$ (A) and C-terminal EF-hand mutant (D1546K) (B) exposed to the indicated Mg_i. (C) Plot of fraction $I_{non\text{-}inact}$ versus log [Mg_i] for WT $Ca_V1.2$ and C-terminal EF-hand mutant (D1546K). Curves represent the best fit of a binding isotherm to the data, with K_D = 0.78 ± 0.04 mM for WT and K_D = 3.6 ± 1.4 mM Mg_i for D1546K.

Comparison of VDI for native and transfected $Ca_V1.2$ channels

Under recording conditions with reduced Mg_i (0.26 mM) and Na^+ as charge carrier, the level of inactivation of $I_{Ca,L}$(Na) in ventricular myocytes was substantially greater than that of $I_{Cav1.2}$(Na) in tsA-201 cells (Fig. 6 A). At 0.26 mM Mg_i, we observed a value of r_{300} of 0.46 ± 0.02 (n = 4) for $I_{Ca,L}$(Na) versus 0.87 ± 0.04 (n = 8) for $Ca_V1.2$(Na) ($P < 0.0001$) (Fig. 6, A and B). Several factors could contribute to the observed difference between the VDI of L-type Ca^{2+} current in ventricular myocytes and $Ca_V1.2$ expressed in tsA-201 cells, including differences in expressed $Ca_V\beta$ subunits (Colecraft et al., 2002) and/or in association with the distal C-terminal regulatory domain (DCRD) (Hulme et al., 2006; see below).

Effect of $Ca_V\beta$ subunits on VDI

$Ca_V\beta$ subunits affect the inactivation properties of $Ca_V1.2$ channels (Catterall, 2000; Colecraft et al., 2002). In agreement with previous work, we found that VDI of $Ca_V1.2$ channels is greater with the $Ca_V\beta_{1b}$ subunit than with the $Ca_V\beta_{2a}$ subunit in the presence of 2.4 mM Mg_i (Fig. 6, C and D). It remains uncertain which $Ca_V\beta$ subunit is predominant in the heart (Foell et al., 2004; Pitt et al., 2006; Ter Keurs and Boyden, 2007), but increasing evidence points to the $Ca_V\beta_2$ family (Gao et al., 1997; Foell et al., 2004; Weissgerber et al., 2006). Previous studies of Ca^{2+} and Ba^{2+} currents suggested that $Ca_V\beta_{2b}$ recapitulates the inactivation profile of L-type currents of ventricular myocytes (Colecraft et al., 2002). We tested the impact of $Ca_V\beta_{2b}$ on VDI of $Ca_V1.2$ expressed in tsA-201 cells, using 0.26 mM Mg_i to minimize its effect on VDI of $Ca_V1.2$ and Na^+ as charge carrier to eliminate any effects of divalent ions on the inactivation process. Under these conditions, $Ca_V\beta_{2b}$ significantly increased VDI compared with $Ca_V\beta_{1b}$ and $Ca_V\beta_{2a}$ (Fig. 6, E–H). Although the expression of $Ca_V\beta_{2b}$ enhanced the inactivation of $Ca_V1.2$ (Na) currents, the level of inactivation is less than previously reported for $Ca_V\beta_{1b}$ and $Ca_V\beta_{2b}$ (Colecraft et al., 2002; Takahashi et al., 2003). This difference is caused by the use of 0.26 mM Mg_i in our experiments because a much larger effect of the $Ca_V\beta_{1b}$ subunit is observed at 2.4 mM Mg_i (Fig. 6, C and D). Nevertheless, the results at 0.26 mM Mg_i show that the $Ca_V\beta$ subunits do not have a profound effect on

TABLE I

Steady-state inactivation parameters of WT $Ca_V1.2$ and D1546K $Ca_V1.2$ EF-hand mutant at different Mg_i concentrations

	WT $Ca_V1.2$				D1546K			
[Mg_i] (mM)	$V_{1/2}$ (mV)	k (mV)	$I_{non\text{-}inact}$[a]	n	$V_{1/2}$ (mV)	k (mV)	$I_{non\text{-}inact}$[a]	n
0.26	−31.6 ± 0.8	9.6 ± 0.7	0.26 ± 0.04	13	−29.8 ± 0.5	9.2 ± 0.5	0.32 ± 0.04	5
0.8	−31.2 ± 0.7	9.4 ± 0.7	0.15 ± 0.04	9	−31.7 ± 1.0	10.2 ± 1.1	0.28 ± 0.04[b]	5
2.4	−36.0 ± 0.2[c]	8.7 ± 0.2	0.05 ± 0.02[d]	4	−36.9 ± 0.8[c]	7.3 ± 0.7	0.22 ± 0.07[b]	8
7.2	−47.3 ± 0.2[c]	9.0 ± 0.1	0.02 ± 0.01[c]	10	−43.4 ± 0.3[c]	6.1 ± 0.3	0.05 ± 0.01[c]	5

[a]Non-inactivating normalized $Ca_V1.2$ (Na) current after a 4-s depolarization at 20 mV.
[b]Values are significantly different from WT; $P < 0.05$.
[c]Values are significantly ($P < 0.01$) different than parameters at 0.26 mM Mg_i.
[d]Values are significantly ($P < 0.05$) different than parameters at 0.26 mM Mg_i.

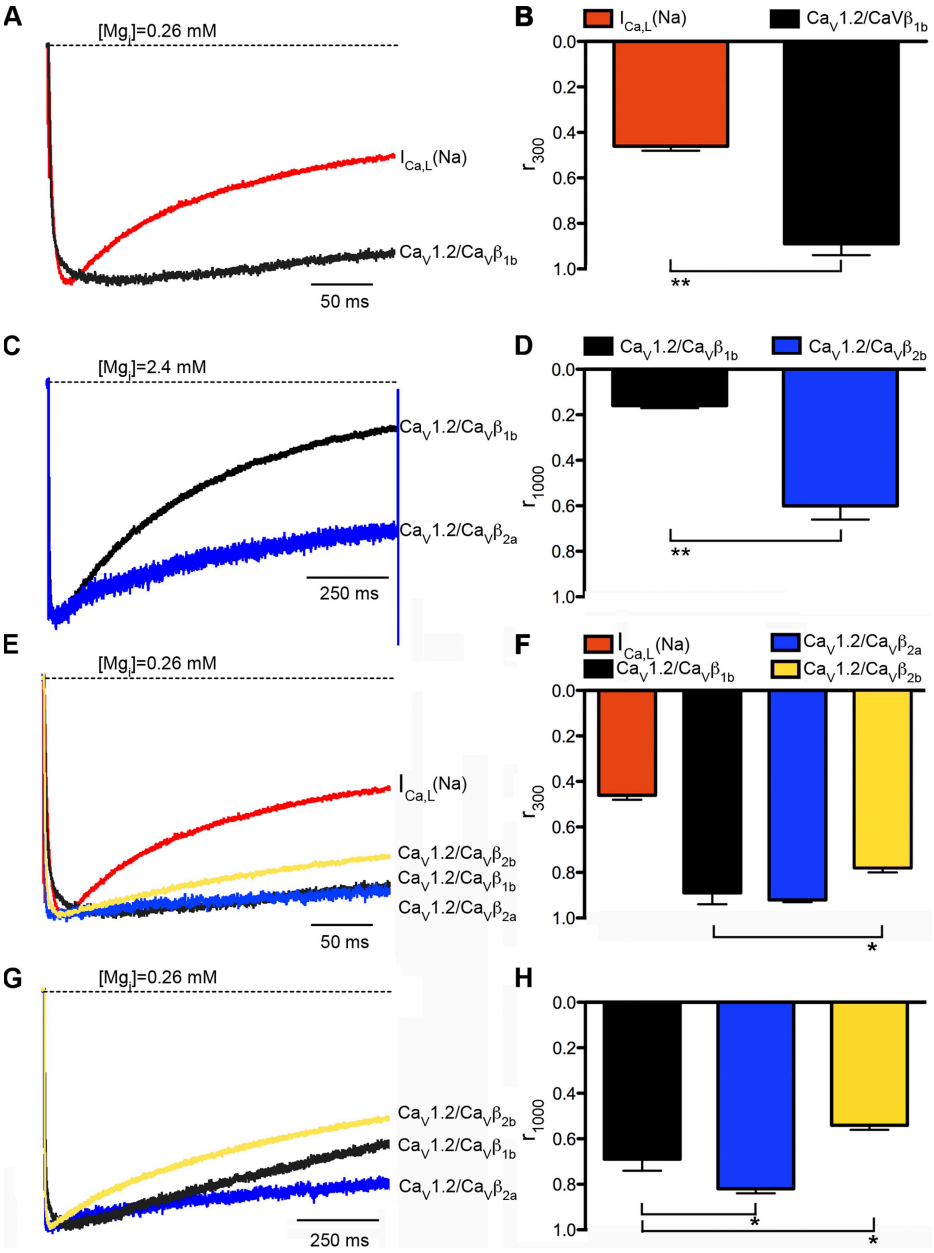

Figure 6. Effects of $Ca_V\beta$ subunits and Mg_i on VDI of $Ca_V1.2$ with Na^+ as charge carrier. (A and B) Comparison of VDI of mouse ventricular myocyte $Ca_V1.2$ current ($I_{Ca,L}$) and current due to $Ca_V1.2$ expressed in tsA-201 cells $I_{CaV1.2}$. (A) Normalized and averaged current traces with Na^+ as charge carrier. (B) Mean r_{300} for $I_{Ca,L}$ ($n = 4$) and $I_{CaV1.2}$ ($n = 7$). Mg_i was 0.26 mM. (C and D) $Ca_V1.2$ and the indicated $Ca_V\beta$ subunits expressed in tsA-201 cells and studied with high (2.4 mM) Mg_i. (C) Mean normalized current traces in response to 1,000-ms depolarizations to 0 mV. (D) Mean r_{1000} for $Ca_V1.2$ expressed with $Ca_V\beta_{1b}$ ($n = 15$) and $Ca_V\beta_{2a}$ ($n = 6$). (E–H) $Ca_V1.2$ and the indicated $Ca_V\beta$ subunits expressed in tsA-201 cells at low (0.26 mM) Mg_i with pulse durations of 300 ms (E and F) and 1,000 ms (G and H). (E and G) Mean normalized currents in response to depolarizations to 0 mV. (E) Mean r_{300} for $Ca_V1.2$ expressed with the indicated β subunits. $Ca_V\beta_{2a}$: $n = 16$; $Ca_V\beta_{2b}$: $n = 10$. Data from ventricular myocytes $I_{Ca,L}$(Na) are replotted for comparison. (H) Mean r_{1000} for $Ca_V1.2$ expressed with $Ca_V\beta_{1b}$, $Ca_V\beta_{2a}$, or $Ca_V\beta_{2b}$.

VDI in the presence of low Mg_i when divalent cation–dependent inactivation is prevented by use of Na^+ as charge carrier, and therefore indicate that $Ca_V\beta$ subunits cannot fully account for the difference in the rate of VDI between L-type Ca^{2+} currents in ventricular myocytes and $Ca_V1.2$ channels expressed in tsA-201 cells illustrated in Fig. 6 A.

Effect of the distal C terminus of $Ca_V1.2$ on VDI

The C termini of $Ca_V1.1$ and $Ca_V1.2$ channels are proteolytically processed in skeletal and cardiac muscle tissues, respectively (De Jongh et al., 1991, 1996; Gerhardstein et al., 2000; Hulme et al., 2005). The proteolytically processed distal C terminus is thought to remain tethered to the proximal C terminus via noncovalent interactions between the DCRD and the proximal C-terminal regulatory domain (PCRD) (Hulme et al., 2006). This interaction has potent autoinhibitory effects on $Ca_V1.2$ currents when the distal C terminus is expressed as a separate protein with truncated $Ca_V1.2$ channels (Hulme et al., 2006). To determine the effect of formation of this complex on VDI, we expressed the truncated $Ca_V1.2$ channel ($Ca_V1.2\Delta1821$) in tsA-201 cells with and without the distal C terminus composed of amino acid residues 1,822–2,171 ($distal_{1822–2171}$). There was no significant difference in inactivation between $Ca_V1.2\Delta1821/Ca_V\beta_{2b}$ (Fig. 7, A and B) and full-length $Ca_V1.2/Ca_V\beta_{2b}$ (Fig. 6, G and H), as the r_{1000} was 0.54 ± 0.03 ($n = 10$) for $Ca_V1.2\Delta1821$ and 0.54 ± 0.03 ($n = 9$) (P = 1.0) for full-length $Ca_V1.2$, respectively. On

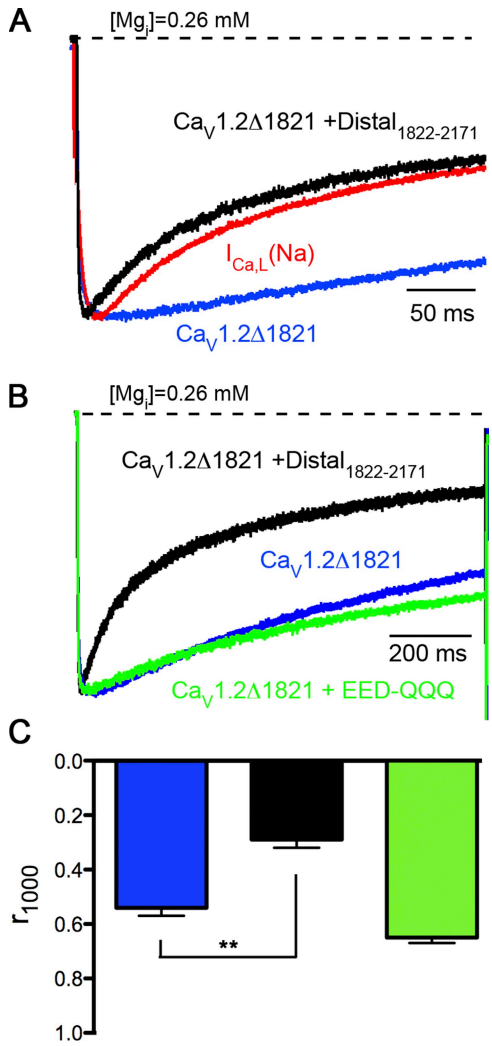

Figure 7. Effect of the distal C terminus of $Ca_V1.2$ on VDI. (A) Mean normalized currents due to expression of the truncated $Ca_V1.2\Delta1821$ α1 subunit alone or with coexpression of the separate distal C terminus ($distal_{1822–2171}$). Data for $I_{Ca,L}$ from ventricular myocytes is shown for comparison. (B) Mean normalized currents due to the truncated $Ca_V1.2\Delta1821$ α1 subunit coexpressed with a mutant distal C terminus containing the triple mutation EED-QQQ compared with currents due to the channel constructs shown in A. (C) Mean r_{1000} for truncated $Ca_V1.2$ expressed alone or with WT or mutant distal C termini (EED-QQQ). $Ca_V\beta_{2b}$ was used in the experiments in this and all subsequent figures. n = $Ca_V1.2\Delta1821$ alone: 10; $Ca_V1.2\Delta1821$ + $distal_{1822–2171}$: 16; $Ca_V1.2\Delta1821$ + EED-QQQ: 10. Mg_i was 0.26 mM.

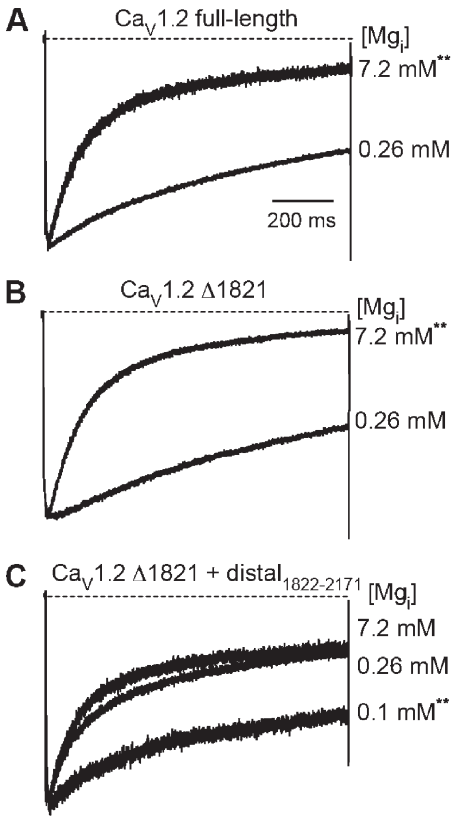

Figure 8. Effects of the distal C terminus on modulation of VDI by Mg_i. Effect of Mg_i on VDI in mean normalized current traces recorded from expression of (A) full-length $Ca_V1.2$, (B) truncated $Ca_V1.2\Delta1821$, and (C) $Ca_V1.2\Delta1821$ coexpressed with $distal_{1822–2171}$. In A, n = 10 and 8 for 0.26 and 7.2 mM Mg_i, respectively. In B, n = 10 and 7. In C, n = 5, 16, and 11 for 0.1, 0.26, and 7.2 mM Mg_i, respectively.

the other hand, the coexpression of $distal_{1822–2171}$ with $Ca_V1.2\Delta1821$ enhanced inactivation compared with $Ca_V1.2\Delta1821$ alone (Fig. 7, A and B), with r_{1000} = 0.54 ± 0.03 (n = 10) for $Ca_V1.2\Delta1821$ versus r_{1000} = 0.28 ± 0.03 (n = 21) for $Ca_V1.2\Delta1821$ with $distal_{1822–2171}$ ($P < 0.01$) (Fig. 7, B and C). VDI of $Ca_V1.2\Delta1821$ with $distal_{1822–2171}$ was similar to VDI of the L-type Ca^{2+} current in ventricular myocytes (Fig. 7 A, $I_{Ca,L}$). These results show that formation of the noncovalent autoinhibitory complex of the distal C-terminal domain with the truncated $Ca_V1.2$ channel greatly enhances VDI. This interaction may contribute to the more rapid rate of VDI observed in ventricular myocytes, where we estimated that at least 48% of $Ca_V1.2$ channels are in the form of proteolytically processed channels with associated C-terminal domain (Hulme et al., 2006).

Because the effect of the distal C terminus on the activity of $Ca_V1.2$ channels is mediated via an electrostatic interaction between two positively charged amino acid residues in the PCRD(RR) and three negatively charged residues (EED) in the DCRD (Hulme et al., 2006), we tested the effect of the DCRD mutant EED-QQQ($Distal_{1822–2171}$), which was shown to significantly reduce the effect of the distal C terminus on the coupling ratio of $Ca_V1.2$ channels (Hulme et al., 2006). Our results show that the EED-QQQ distal C-terminal mutant does not enhance VDI of $Ca_V1.2\Delta1821$ (Fig. 7, B and C), suggesting that the electrostatic interaction between the PCRD and DCRD is important in mediating the effect of the distal C terminus on VDI of $Ca_V1.2$ channels. This effect of the C terminus was not dependent on the $Ca_V\beta$ subunit expressed, as similar observations were made with $Ca_V\beta_{1b}$ subunit (unpublished

data). These effects of distal$_{1822–2171}$ on VDI of Ca$_V$1.2Δ1821 are consistent with previous results showing that distal$_{1822–2171}$ reduces the current amplitude of Ca$_V$1.2Δ1821 through interaction with the EED motif in the DCRD (Hulme et al., 2006). Overall, these results suggest that the increased VDI of L-type Ca^{2+} current in cardiac myocytes results at least in part from the interaction with distal C terminus of Ca$_V$1.2, which enhances VDI of Ca$_V$1.2 channels through electrostatic interactions with the PCRD.

Cooperative modulation of VDI by the distal C terminus and Mg$_i$

Because both the distal C terminus and Mg$_i$ enhance inactivation of Ca$_V$1.2 channels, we examined the impact of the distal C terminus on the Mg$_i$ modulation of VDI of truncated Ca$_V$1.2 channels. As in previous work, Mg$_i$ enhanced the inactivation of the full-length Ca$_V$1.2 channel (Fig. 8 A) (Brunet et al., 2005a), with r_{1000} = 0.54 ± 0.03 for 0.26 mM versus 0.15 ± 0.03 for 7.2 mM Mg$_i$ ($P < 0.001$). Similar to the Mg$_i$ effect on full-length channels, Mg$_i$ also enhanced VDI of Ca$_V$1.2Δ1821 (Fig. 8 B). The r_{1000} value was 0.54 ± 0.03 at 0.26 mM Mg$_i$ versus 0.10 ± 0.05 ($P < 0.001$) for 7.2 mM Mg$_i$. In contrast, when distal$_{1822–2171}$ was coexpressed with Ca$_V$1.2Δ1821 channels, 7.2 mM Mg$_i$ did not significantly enhance VDI of Ca$_V$1.2 (Fig. 8 C; 0.26 mM, r_{1000} = 0.28 ± 0.03; 7.2 mM, r_{1000} = 0.25 ± 0.03; $P = 0.52$). To determine whether reduced Mg$_i$ regulates this autoinhibitory complex, a lower Mg$_i$ concentration (0.1 mM) was tested. The dialysis of 0.1 mM Mg$_i$ reduced inactivation (r_{1000} = 0.60 ± 0.05; $P < 0.01$) compared with 0.26 and 7.2 mM Mg$_i$ (Fig. 8 C). This result suggests that the noncovalent interaction of the distal C terminus with the Ca$_V$1.2 channel enhances regulation of VDI by Mg$_i$, possibly by increasing the affinity for binding of Mg$_i$ to the proximal C-terminal EF-hand.

Requirement for the EF-hand of Ca$_V$1.2 for regulation of VDI by the distal C terminus

The effect of the distal C-terminal domain on the rate of VDI can be clearly observed by comparing the rate of inactivation for Ca$_V$1.2Δ1821 without and with distal$_{1822–2171}$ at 0.26 mM Mg$_i$ (Fig. 7, A and B). A similar effect on VDI is observed for truncation at position 1,800 (Fig. 9 A), the probable point of in vivo proteolytic processing determined by mass spectrometric analysis of the related Ca$_V$1.1 channel (Hulme et al., 2005), and more extensive analysis has shown that these two forms of the autoinhibitory Ca$_V$1.2 channel complex cleaved at position 1,800 or 1,821 have nearly identical functional properties when studied side-by-side (unpublished data). To determine the role of the proximal C-terminal EF-hand in the enhancement of VDI by the distal C terminus in Ca$_V$1.2Δ1800, we studied the mutation D1546R, which reduces the effects of Mg$_i$ on current amplitude and VDI of Ca$_V$1.2 (Brunet et al., 2005a,b). With EF-hand mutant Ca$_V$1.2Δ1800(D1546R) plus distal$_{1801–2171}$, the distal C terminus did not enhance VDI of Ca$_V$1.2 (Fig. 9 B) in contrast to Ca$_V$1.2Δ1800 with

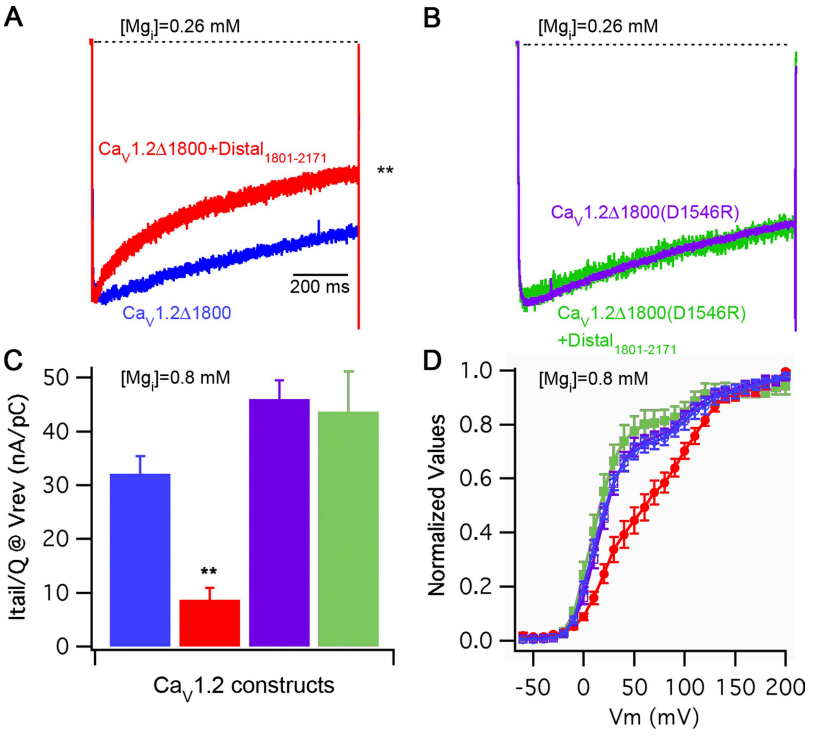

Figure 9. Requirement for a functional proximal C-terminal EF-hand for the effects of the distal C terminus on Ca$_V$1.2 current. Effect of coexpression of distal$_{1801–2171}$ on mean normalized Na^+ currents resulting from expression of (A) Ca$_V$1.2Δ1800 or (B) Ca$_V$1.2Δ1800 containing mutation D1546R in the EF-hand (Ca$_V$1.2Δ1800(D1546R)). n = 15, 17, 10, and 15 for Ca$_V$1.2Δ1800(D1546R), Ca$_V$1.2Δ1800(D1546R) plus distal$_{1801–2171}$, Ca$_V$1.2Δ1800, and Ca$_V$1.2Δ1800 plus distal$_{1801–2171}$, respectively. Mg$_i$ was 0.26 mM. (C) Mean coupling ratios measured as the ratio of peak tail current at −40 mV (nA) after a depolarization to the reversal potential and gating charge movement measured at the reversal potential (pC). Gating charge movement was measured by applying a series of test pulses from the HP of −80 mV to potentials between +60 and 80 mV in 2-mV increments and integrating the gating charge movement at the reversal potential for the ionic current (Hulme et al., 2006). n = 10, 9, 11, and 8. (D) Normalized conductance–voltage relationships. Peak tail currents were measured upon repolarization to −40 mV after 20-ms depolarization to potentials between −40 and 200 mV. Ba^{2+} was used as charge carrier, and Mg$_i$ was 0.8 mM for the experiments in C and D.

WT distal$_{1801–2171}$ (Fig. 9 A). These results indicate that interaction of Mg_i with the EF-hand in the proximal C terminal is required for regulation of VDI by the distal C-terminal domain.

The distal C-terminal domain inhibits $Ca_V1.2$ channel activity by positively shifting the voltage dependence of activation and reducing the coupling ratio of gating charge movement to channel opening (Hulme et al., 2006). Using Ba^{2+} as a charge carrier to allow comparison of our results with the previous work, we found that the D1546R mutation in the EF-hand in the proximal C-terminal domain prevented both the reduction of the coupling ratio (Fig. 9 C) and the positive shift in the voltage dependence of activation of $Ca_V1.2\Delta1800$ (Fig. 9 D). These results demonstrate that a functional EF-hand in the proximal C-terminal domain is required to mediate all of the effects of the noncovalently associated distal C terminus on $Ca_V1.2$ channels, including increased VDI, positively shifted activation, and reduced coupling ratio.

DISCUSSION

Cation-dependent inactivation and Ba^{2+} as charge carrier

We found that use of Ba^{2+} as a charge carrier resulted in a significant level of cation-dependent inactivation of $Ca_V1.2$ channels. In our transfected cell system, we observed a correlation between Ba^{2+} current amplitude and r_{1000} as an index of inactivation. This result is in agreement with previous work (Zhang et al., 1994; Ferreira et al., 1997; Sun et al., 2000), including previous studies of cation-dependent inactivation of $Ca_V1.2$ channels expressed in tsA-201 cells by Ba^{2+} (Ferreira et al., 1997). It was proposed that Ba^{2+} could bind weakly to the same sensor as Ca^{2+}, which is now known to be calmodulin, and could activate the same inactivation mechanism when high local concentrations are achieved (Sun et al., 2000). Based on our results and this previous work, it is evident that unambiguous measurement of VDI requires use of Na^+ or another monovalent cation as charge carrier, taking advantage of the ability of Ca^{2+} channels to conduct monovalent cations with high efficiency in the presence of low extracellular concentrations of Ca^{2+}. Because Ca^{2+}-dependent inactivation is much faster than VDI for $Ca_V1.2$ channels, a small contamination by this cation-dependent inactivation mechanism can have a major impact on measurements of VDI. In addition, in transfected cell systems that yield variable expression of $Ca_V1.2$ channels from different transfections and from different mutants, elimination of cation-dependent inactivation that varies with channel density is especially important. For these reasons, we used Na^+ as permeant ion for most of our experiments on VDI reported here.

Mg_i reduces peak amplitude and increases VDI of native cardiac L-type Ca^{2+} currents at physiological concentrations

Previous reports have suggested that Mg_i could reduce peak L-type Ca^{2+} currents and enhance the VDI in ventricular myocytes, as measured with Ba^{2+} as the permeant ion, (Hartzell and White, 1989; Yamaoka and Seyama, 1996b; Wang et al., 2004). However, it was uncertain whether the Ba^{2+}-dependent inactivation observed in our experiments in transfected cells might contribute substantially to those effects in ventricular myocytes. Our present results with Na^+ as permeant ion clearly demonstrate that, in the absence of permeant divalent ions, increases in Mg_i concentration both reduce peak Ca^{2+} current and enhance VDI in native ventricular myocytes.

Mg_i is ~0.8 mM in intact cardiac myocytes under physiological conditions (Murphy et al., 1989; Headrick and Willis, 1991; Haigney et al., 1998). There is a two- to threefold increase in Mg_i in ventricular myocytes as ATP levels decrease during transient ischemia (Murphy et al., 1989; Headrick and Willis, 1991). Similar two- to threefold increases in Mg_i are observed in cerebral ischemia (Brooks and Bachelard, 1989; Helpern et al., 1993; Williams and Smith, 1995) and in traumatic brain injury (decrease Mg_i) (Vink et al., 1988; Heath and Vink, 1996). In contrast, a decrease of two- to threefold in Mg_i is observed in heart failure (Haigney et al., 1998). Our results show that both the peak amplitude and VDI of L-type Ca^{2+} currents in ventricular myocytes would be substantially regulated by these changes in Mg_i. In heart failure, reduction of Mg_i would increase Ca^{2+} currents and slow their inactivation, which may contribute to dysregulation of Ca^{2+} signaling, hypertrophy, and cytotoxicity. In ischemia, the increase in Mg_i would reduce L-type Ca^{2+} current by reducing peak current and by enhancing VDI. These effects would reduce cytotoxicity caused by Ca^{2+} overload under ischemic conditions. Moreover, this regulatory mechanism would be cell autonomous, reducing Ca^{2+} currents only in those individual cardiac myocytes that are ischemic, while leaving neighboring cells with normal ATP levels uninhibited. This unique cell-autonomous protective mechanism may contribute significantly to preventing Ca^{2+} overload in ischemia.

Upon maintained depolarization, the cardiac L-type calcium current inactivates by dual mechanisms dependent on Ca^{2+} and voltage (Lee et al., 1985; Nilius and Benndorf, 1986). Calcium-dependent inactivation accelerates the decay of the calcium current as calcium accumulates inside the cell during the action potential, and these changes in inactivation kinetics play an important role in the control of action potential duration and excitation–contraction coupling (Kleiman and Houser, 1988; Keung, 1989). However, Ca^{2+}-dependent inactivation does not reduce the peak Ca^{2+} current until after

Ca^{2+} overload has occurred and is not able by itself to reduce the Ca^{2+} current to zero, even at high Ca^{2+} levels. In contrast, VDI can reduce the peak Ca^{2+} current in response to sustained depolarization, even before Ca^{2+} overload has occurred, and it is powerful enough to reduce the Ca^{2+} current to zero as shown in our records. Thus, we propose that in ischemic conditions with sustained membrane depolarization, Mg_i can reduce Ca^{2+} entry via L-type $Ca_V1.2$ channels before Ca^{2+} overload occurs and sustain inhibition as Ca^{2+} is sequestered and pumped out of the cytosol.

Effects of PKA stimulation on Mg_i regulation of L-type Ca^{2+} channels

Previous studies have shown that Mg_i modulation of the cardiac L-type Ca^{2+} channel depends on the state of activation of channels by cAMP-dependent phosphorylation (White and Hartzell, 1988; Wang et al., 2004; Wang and Berlin, 2006). These investigators concluded that the actions of Mg_i to reduce peak currents and enhance VDI are mediated by a separate mechanism from protein phosphorylation, but the extent of modulation by Mg_i is dependent on the phosphorylation state of the $Ca_V1.2$ channel. These conclusions are consistent with the work we present here, in which we find that the effects of Mg_i on peak current and on VDI are caused by the binding of Mg to the C-terminal EF-hand. In other experiments (unpublished data), we found that PKA inhibitors reduced $Ca_V1.2$ current ~50% under our basal physiological conditions; therefore, our results presented here reflect the effects of Mg_i on $Ca_V1.2$ channels whose activity is partially up-regulated by basal cAMP-dependent phosphorylation.

Mg_i enhances VDI of $Ca_V1.2$ channels

Our results show that altering Mg_i has striking effects on VDI of $Ca_V1.2$ channels expressed in tsA-201 cells in the absence of other cardiac-specific proteins. The rate and extent of VDI increase dramatically with increased Mg_i. This enhancement of inactivation occurs with an apparent K_d of 0.9 mM. $Ca_V1.2$ is the predominant Ca^{2+} channel in cardiac cells, and this value falls in the range of normal physiological levels of Mg_i in cardiac cells (0.6–1.0 mM) (Murphy et al., 1989; Headrick and Willis, 1991; Haigney et al., 1998). Thus, the dependence of peak current amplitude and VDI of $Ca_V1.2$ channel on Mg_i that we have defined in the tsA-201 cell expression system likely reflects the Mg_i dependence of peak current amplitude and VDI of the $Ca_V1.2$ channel in vivo.

The proximal C-terminal EF-hand mediates the effects of Mg_i on VDI

Our previous studies of the effects of Mg_i on peak Ca^{2+} currents showed that EF-hand mutations at the −z position (D1546A/NS/K/R) reduce the inhibitory effects of Mg_i because of a decrease in apparent affinity for Mg_i (Brunet et al., 2005b). Our present results extend those findings to VDI and lead to the conclusion that both the

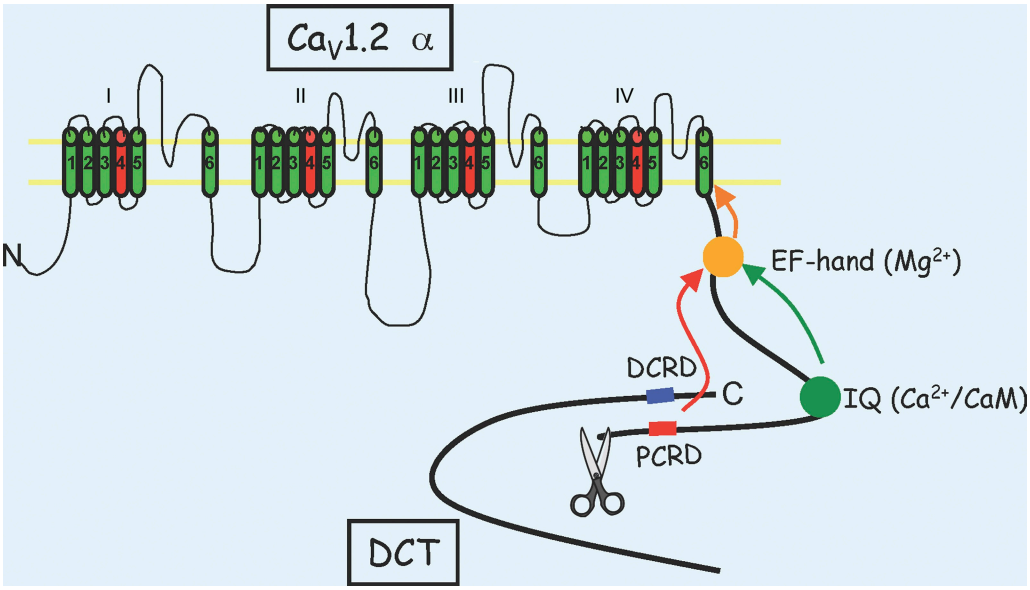

Figure 10. Schematic illustration of the $Ca_V1.2$ α subunit emphasizing the spatial relationship of key regulatory sites located at the proximal C terminus. $Ca_V1.2$, α subunit composed of the N terminus, the four homologous domains with six transmembrane segments, and a reentrant pore loop in each (I–IV), and the C-terminus. The arrows point to the conformational interactions between the distal C terminus (DCT; red arrow) and the IQ motif (Ca^{2+}/CaM) (orange arrow) independently converging on the EF-hand motif (Mg^{2+}), which subsequently may modify the conformation of domain IV S6 segment of the $Ca_V1.2$ α subunit to alter channel-gating properties. The scissors illustrate the site of proteolytic cleavage. CaM, calmodulin.

reduction of peak current amplitude and the enhancement of VDI caused by Mg_i result from its interaction with the proximal C-terminal EF-hand motif. This conclusion is in agreement with previous work suggesting that the structure of the EF-hand of $Ca_V1.2$ is important for VDI (Bernatchez et al., 1998). Evidently, the functional role of the EF-hand in VDI depends on its binding of Mg_i as shown here.

Noncovalent association of the distal C-terminal domain increases the rate of VDI in transfected cells

Although our results describing the modulation of Mg_i on L-type Ca^{2+} current in myocytes are qualitatively similar to our results on Mg_i modulation of $Ca_V1.2$ channels in tsA-201 cells, there are some important quantitative differences. First, Mg_i was more effective at enhancing the inactivation of $Ca_V1.2$ in tsA-201 cells compared with the inactivation of the L-type Ca^{2+} current in ventricular myocytes. Second, VDI was greater for $Ca_V1.2$ channels in cardiac myocytes than for $Ca_V1.2$ expressed in tsA-201 cells, as reported previously using Ba^{2+} as permeant ion (Colecraft et al., 2002). Subunit structure and composition of $Ca_V1.2$ channels in ventricular myocytes and $Ca_V1.2$ channels in tsA-201 cells may contribute to these differences.

Our results show that $Ca_V\beta$s have small but significant effects on the VDI of $Ca_V1.2$ measured with Na^+ as the permeant ion in the presence of low Mg_i. These effects of $Ca_V\beta$s on VDI are smaller than in previous work, and $Ca_V\beta_{2b}$ did not fully restore VDI of $Ca_V1.2$ as reported previously (Colecraft et al., 2002). Our results indicate that $Ca_V\beta$s cannot fully account for the difference in VDI between $Ca_V1.2$ channels in ventricular myocytes and $Ca_V1.2$ channels in transfected cells in the absence of permeant divalent cations.

In myocytes, the distal C terminus of $Ca_V1.2$ is proteolytically processed in situ, whereas it is not cleaved in tsA-201 cells (De Jongh et al., 1991, 1994, 1996; Hulme et al., 2005). Our results demonstrate that expression of the distal C terminus of $Ca_V1.2$ together with the truncated $Ca_V1.2\Delta1821$ channel markedly enhanced VDI under our recording conditions. This enhancement of VDI was blocked by the distal C terminus mutation EED-QQQ, supporting a role for an electrostatic interaction between the PCRD and DCDR in mediating the effect of the distal C terminus on VDI. This effect of the distal C terminus on VDI was greater than the effects of $Ca_V\beta$s tested, but it was comparable to the effects of Mg_i. These findings support an important role of the distal C-terminal domain in regulating Ca^{2+} currents via control of coupling ratio, voltage-dependent activation, and VDI. These results are consistent with the autoinhibitory function demonstrated for the distal C terminus of $Ca_V1.2$ in previous studies (Hulme et al., 2006).

Mg_i and the proximal C-terminal EF-hand are required for the functional effects of the noncovalently associated distal C-terminal domain

Because the effect of the distal C terminus on VDI was comparable in amplitude to that of Mg_i, we investigated the possible functional interaction between Mg_i and the distal C terminus. To our surprise, when the distal C terminus was expressed together with the cleaved $Ca_V1.2$ channel, increasing Mg_i concentration from 0.26 to 7.2 mM had little effect. On the other hand, decreasing Mg_i to lower levels reduced VDI, indicating that the apparent affinity for Mg_i was increased by noncovalent association of the distal C terminus. These results demonstrate a cooperative interaction between the distal C terminus and Mg_i binding to the proximal C-terminal EF-hand motif in enhancement of VDI. Consistent with this idea, the mutation D1546R reduces affinity for the binding of Mg_i to the proximal C-terminal EF-hand and reduces the functional effects of the distal C terminus. Overall, these results place the EF-hand as a downstream structural element through which the distal C terminus regulates VDI of $Ca_V1.2$ channels. Evidently, Mg_i enhancement of VDI is cooperatively coupled to enhancement of VDI by the distal C terminus.

A C-terminal signaling complex controlling inactivation of $Ca_V1.2$ channels

The inactivation of $Ca_V1.2$ channels is both Ca^{2+} and voltage dependent. Our results show that VDI of $Ca_V1.2$ channels is regulated by the distal C terminus, Mg_i, and the proximal C-terminal EF-hand. At the same time, Ca^{2+}-dependent inactivation of $Ca_V1.2$ channels is regulated by the binding of Ca^{2+} and calmodulin to an IQ motif just downstream from the EF-hand motif in the proximal C-terminal domain (Peterson et al., 1999; Zuhlke et al., 2000; Pitt et al., 2001; Ohrtman et al., 2008), and the effects of Ca^{2+}/calmodulin binding to the IQ motif on CDI are blocked by mutations on the external, non-cation–binding face of the EF-hand (Peterson et al., 2000). The spatial relationship of these regulatory sites is illustrated in Fig. 10, which emphasizes that regulatory influences on both Ca^{2+}-dependent inactivation and VDI from downstream in the C-terminal domain are mediated via the proximal C-terminal EF-hand and are potentially influenced by the binding of Mg_i. We propose that conformational changes induced by noncovalent association of the distal C-terminal domain and Ca^{2+}/calmodulin with the proximal C-terminal domain are propagated from the regulatory regions of the C terminus to the pore-lining IVS6 segment via the EF-hand motif. These results further emphasize the interactive nature of the multiple regulatory elements in the C terminus of $Ca_V1.2$ channels, and place Mg_i binding to the proximal C-terminal EF-hand motif in position to serve as a key integrator of multiple regulatory signals that control Ca^{2+} channel function.

The authors thank Dr. Matthew Fuller (Department of Pharmacology, University of Washington) for determining the functional properties of $Ca_V1.2a\Delta1800$.

The authors gratefully acknowledge the financial support provided by a National Scientist Development Grant from the American Heart Association to S. Brunet and the National Institutes of Health (P01 HL 44948 and R01 HL085372) to W.A. Catterall.

Angus C. Nairn served as editor.

Submitted: 27 January 2009
Accepted: 25 June 2009

REFERENCES

Agus, Z.S., E. Kelepouris, I. Dukes, and M. Morad. 1989. Cytosolic magnesium modulates calcium channel activity in mammalian ventricular cells. *Am. J. Physiol.* 256:C452–C455.

Ahmmed, G.U., P.H. Dong, G. Song, N.A. Ball, Y. Xu, R.A. Walsh, and N. Chiamvimonvat. 2000. Changes in Ca^{2+} cycling proteins underlie cardiac action potential prolongation in a pressure-overloaded guinea pig model with cardiac hypertrophy and failure. *Circ. Res.* 86:558–570.

Almers, W., E.W. McCleskey, and P.T. Palade. 1984. A non-selective cation conductance in frog muscle membrane blocked by micromolar external calcium ions. *J. Physiol.* 353:565–583.

Ashcroft, F.M., and P.R. Stanfield. 1981. Calcium dependence of the inactivation of calcium currents in skeletal muscle fibers of an insect. *Science.* 213:224–226.

Bernatchez, G., D. Talwar, and L. Parent. 1998. Mutations in the EF-hand motif impair the inactivation of barium currents of the cardiac α1C channel. *Biophys. J.* 75:1727–1739.

Bers, D.M. 2002. Cardiac excitation-contraction coupling. *Nature.* 415:198–205.

Brehm, P., and R. Eckert. 1978. Calcium entry leads to inactivation of calcium channel in Paramecium. *Science.* 202:1203–1206.

Brooks, K.J., and H.S. Bachelard. 1989. Changes in intracellular free magnesium during hypoglycaemia and hypoxia in cerebral tissue as calculated from ^{31}P-nuclear magnetic resonance spectra. *J. Neurochem.* 53:331–334.

Brunet, S., F. Aimond, H. Li, W. Guo, J. Eldstrom, D. Fedida, K.A. Yamada, and J.M. Nerbonne. 2004. Heterogeneous expression of repolarizing, voltage-gated K^+ currents in adult mouse ventricles. *J. Physiol.* 559:103–120.

Brunet, S., T. Scheuer, and W.A. Catterall. 2005a. Intracellular magnesium enhances voltage-dependent inactivation of $Ca_V1.2$ by binding to the C-terminal EF-hand. *Biophys. Soc. Abst.* 976-Plat.

Brunet, S., T. Scheuer, R. Klevit, and W.A. Catterall. 2005b. Modulation of $Ca_V1.2$ channels by Mg^{2+} acting at an EF-hand motif in the COOH-terminal domain. *J. Gen. Physiol.* 126:311–323.

Catterall, W.A. 2000. Structure and regulation of voltage-gated Ca^{2+} channels. *Annu. Rev. Cell Dev. Biol.* 16:521–555.

Colecraft, H.M., B. Alseikhan, S.X. Takahashi, D. Chaudhuri, S. Mittman, V. Yegnasubramanian, R.S. Alvania, D.C. Johns, E. Marban, and D.T. Yue. 2002. Novel functional properties of Ca^{2+} channel β subunits revealed by their expression in adult rat heart cells. *J. Physiol.* 541:435–452.

De Jongh, K.S., C. Warner, A.A. Colvin, and W.A. Catterall. 1991. Characterization of the two size forms of the α 1 subunit of skeletal muscle L-type calcium channels. *Proc. Natl. Acad. Sci. USA.* 88:10778–10782.

De Jongh, K.S., A.A. Colvin, K.K. Wang, and W.A. Catterall. 1994. Differential proteolysis of the full-length form of the L-type calcium channel α 1 subunit by calpain. *J. Neurochem.* 63:1558–1564.

De Jongh, K.S., B.J. Murphy, A.A. Colvin, J.W. Hell, M. Takahashi, and W.A. Catterall. 1996. Specific phosphorylation of a site in the full-length form of the α 1 subunit of the cardiac L-type calcium channel by adenosine 3′,5′-cyclic monophosphate-dependent protein kinase. *Biochemistry.* 35:10392–10402.

Ferreira, G., J. Yi, E. Rios, and R. Shirokov. 1997. Ion-dependent inactivation of barium current through L-type calcium channels. *J. Gen. Physiol.* 109:449–461.

Foell, J.D., R.C. Balijepalli, B.P. Delisle, A.M. Yunker, S.L. Robia, J.W. Walker, M.W. McEnery, C.T. January, and T.J. Kamp. 2004. Molecular heterogeneity of calcium channel β-subunits in canine and human heart: evidence for differential subcellular localization. *Physiol. Genomics.* 17:183–200.

Gao, T., T.S. Puri, B.L. Gerhardstein, A.J. Chien, R.D. Green, and M.M. Hosey. 1997. Identification and subcellular localization of the subunits of L-type calcium channels and adenylyl cyclase in cardiac myocytes. *J. Biol. Chem.* 272:19401–19407.

Gerhardstein, B.L., T. Gao, M. Bunemann, T.S. Puri, A. Adair, H. Ma, and M.M. Hosey. 2000. Proteolytic processing of the C terminus of the α(1C) subunit of L-type calcium channels and the role of a proline-rich domain in membrane tethering of proteolytic fragments. *J. Biol. Chem.* 275:8556–8563.

Hadley, R.W., and J.R. Hume. 1987. An intrinsic potential-dependent inactivation mechanism associated with calcium channels in guinea-pig myocytes. *J. Physiol.* 389:205–222.

Haigney, M.C., S. Wei, S. Kaab, E. Griffiths, R. Berger, R. Tunin, D. Kass, W.G. Fisher, B. Silver, and H. Silverman. 1998. Loss of cardiac magnesium in experimental heart failure prolongs and destabilizes repolarization in dogs. *J. Am. Coll. Cardiol.* 31:701–706.

Hartzell, H.C., and R.E. White. 1989. Effects of magnesium on inactivation of the voltage-gated calcium current in cardiac myocytes. *J. Gen. Physiol.* 94:745–767.

Headrick, J.P., and R.J. Willis. 1991. Cytosolic free magnesium in stimulated, hypoxic, and underperfused rat heart. *J. Mol. Cell. Cardiol.* 23:991–999.

Heath, D.L., and R. Vink. 1996. Traumatic brain axonal injury produces sustained decline in intracellular free magnesium concentration. *Brain Res.* 738:150–153.

Helpern, J.A., A.M. Vande Linde, K.M. Welch, S.R. Levine, L.R. Schultz, R.J. Ordidge, H.R. Halvorson, and J.W. Hugg. 1993. Acute elevation and recovery of intracellular $[Mg^{2+}]$ following human focal cerebral ischemia. *Neurology.* 43:1577–1581.

Hess, P., and R.W. Tsien. 1984. Mechanism of ion permeation through calcium channels. *Nature.* 309:453–456.

Hulme, J.T., T.W. Lin, R.E. Westenbroek, T. Scheuer, and W.A. Catterall. 2003. β-adrenergic regulation requires direct anchoring of PKA to cardiac $Ca_V1.2$ channels via a leucine zipper interaction with A kinase-anchoring protein 15. *Proc. Natl. Acad. Sci. USA.* 100:13093–13098.

Hulme, J.T., K. Konoki, T.W. Lin, M.A. Gritsenko, D.G. Camp II, D.J. Bigelow, and W.A. Catterall. 2005. Sites of proteolytic processing and noncovalent association of the distal C-terminal domain of $Ca_V1.1$ channels in skeletal muscle. *Proc. Natl. Acad. Sci. USA.* 102:5274–5279.

Hulme, J.T., V. Yarov-Yarovoy, T.W. Lin, T. Scheuer, and W.A. Catterall. 2006. Autoinhibitory control of the $Ca_V1.2$ channel by its proteolytically processed distal C-terminal domain. *J. Physiol.* 576:87–102.

Keung, E.C. 1989. Calcium current is increased in isolated adult myocytes from hypertrophied rat myocardium. *Circ. Res.* 64:753–763.

Kleiman, R.B., and S.R. Houser. 1988. Calcium currents in normal and hypertrophied isolated feline ventricular myocytes. *Am. J. Physiol.* 255:H1434–H1442.

Lee, K.S., E. Marban, and R.W. Tsien. 1985. Inactivation of calcium channels in mammalian heart cells: joint dependence on membrane potential and intracellular calcium. *J. Physiol.* 364:395–411.

Mendez, D.R., R. Corbett, C. Macias, and A. Laptook. 2005. Total and ionized plasma magnesium concentrations in children after traumatic brain injury. *Pediatr. Res.* 57:347–352.

Mikami, A., K. Imoto, T. Tanabe, T. Niidome, Y. Mori, H. Takeshima, S. Narumiya, and S. Numa. 1989. Primary structure and functional expression of the cardiac dihydropyridine-sensitive calcium channel. *Nature.* 340:230–233.

Murphy, E., C. Steenbergen, L.A. Levy, B. Raju, and R.E. London. 1989. Cytosolic free magnesium levels in ischemic rat heart. *J. Biol. Chem.* 264:5622–5627.

Nilius, B., and K. Benndorf. 1986. Joint voltage- and calcium dependent inactivation of Ca channels in frog atrial myocardium. *Biomed. Biochim. Acta.* 45:795–811.

Ohrtman, J., B. Ritter, A. Polster, K.G. Beam, and S. Papadopoulos. 2008. Sequence differences in the IQ motifs of $Ca_V1.1$ and $Ca_V1.2$ strongly impact calmodulin binding and calcium-dependent inactivation. *J. Biol. Chem.* 283:29301–29311.

Pelzer, S., C. La, and D.J. Pelzer. 2001. Phosphorylation-dependent modulation of cardiac calcium current by intracellular free magnesium. *Am. J. Physiol. Heart Circ. Physiol.* 281:H1532–H1544.

Peterson, B.Z., C.D. DeMaria, J.P. Adelman, and D.T. Yue. 1999. Calmodulin is the Ca^{2+} sensor for Ca^{2+}-dependent inactivation of L-type calcium channels. *Neuron.* 22:549–558.

Peterson, B.Z., J.S. Lee, J.G. Mulle, Y. Wang, M. de Leon, and D.T. Yue. 2000. Critical determinants of Ca^{2+}-dependent inactivation within an EF-hand motif of L-type Ca^{2+} channels. *Biophys. J.* 78:1906–1920.

Pitt, G.S., R.D. Zuhlke, A. Hudmon, H. Schulman, H. Reuter, and R.W. Tsien. 2001. Molecular basis of calmodulin tethering and Ca^{2+}-dependent inactivation of L-type Ca^{2+} channels. *J. Biol. Chem.* 276:30794–30802.

Pitt, G.S., W. Dun, and P.A. Boyden. 2006. Remodeled cardiac calcium channels. *J. Mol. Cell. Cardiol.* 41:373–388.

Resnick, L.M., M. Barbagallo, M. Bardicef, O. Bardicef, Y. Sorokin, J. Evelhoch, L.J. Dominguez, B.A. Mason, and D.B. Cotton. 2004. Cellular-free magnesium depletion in brain and muscle of normal and preeclamptic pregnancy: a nuclear magnetic resonance spectroscopic study. *Hypertension.* 44:322–326.

Reuter, H. 1979. Properties of two inward membrane currents in the heart. *Annu. Rev. Physiol.* 41:413–424.

Splawski, I., K.W. Timothy, L.M. Sharpe, N. Decher, P. Kumar, R. Bloise, C. Napolitano, P.J. Schwartz, R.M. Joseph, K. Condouris, et al. 2004. $Ca_V1.2$ calcium channel dysfunction causes a multisystem disorder including arrhythmia and autism. *Cell.* 119:19–31.

Splawski, I., K.W. Timothy, N. Decher, P. Kumar, F.B. Sachse, A.H. Beggs, M.C. Sanguinetti, and M.T. Keating. 2005. Severe arrhythmia disorder caused by cardiac L-type calcium channel mutations. *Proc. Natl. Acad. Sci. USA.* 102:8089–8096.

Sun, L., J.S. Fan, J.W. Clark, and P.T. Palade. 2000. A model of the L-type Ca^{2+} channel in rat ventricular myocytes: ion selectivity and inactivation mechanisms. *J. Physiol.* 529:139–158.

Takahashi, S.X., S. Mittman, and H.M. Colecraft. 2003. Distinctive modulatory effects of five human auxiliary β2 subunit splice variants on L-type calcium channel gating. *Biophys. J.* 84:3007–3021.

Ter Keurs, H.E., and P.A. Boyden. 2007. Calcium and arrhythmogenesis. *Physiol. Rev.* 87:457–506.

Tillotson, D. 1979. Inactivation of Ca conductance dependent on entry of Ca ions in molluscan neurons. *Proc. Natl. Acad. Sci. USA.* 76:1497–1500.

Vink, R., T.K. McIntosh, P. Demediuk, M.W. Weiner, and A.I. Faden. 1988. Decline in intracellular free Mg^{2+} is associated with irreversible tissue injury after brain trauma. *J. Biol. Chem.* 263:757–761.

Wang, M., and J.R. Berlin. 2006. Channel phosphorylation and modulation of L-type Ca^{2+} currents by cytosolic Mg^{2+} concentration. *Am. J. Physiol. Cell Physiol.* 291:C83–C92.

Wang, M., M. Tashiro, and J.R. Berlin. 2004. Regulation of L-type calcium current by intracellular magnesium in rat cardiac myocytes. *J. Physiol.* 555:383–396.

Weissgerber, P., B. Held, W. Bloch, L. Kaestner, K.R. Chien, B.K. Fleischmann, P. Lipp, V. Flockerzi, and M. Freichel. 2006. Reduced cardiac L-type Ca^{2+} current in $Ca_V\beta2-/-$ embryos impairs cardiac development and contraction with secondary defects in vascular maturation. *Circ. Res.* 99:749–757.

White, R.E., and H.C. Hartzell. 1988. Effects of intracellular free magnesium on calcium current in isolated cardiac myocytes. *Science.* 239:778–780.

Williams, G.D., and M.B. Smith. 1995. Application of the accurate assessment of intracellular magnesium and pH from the ^{31}P shifts of ATP to cerebral hypoxia-ischemia in neonatal rat. *Magn. Reson. Med.* 33:853–857.

Yamaoka, K., and I. Seyama. 1996a. Modulation of Ca^{2+} channels by intracellular Mg^{2+} ions and GTP in frog ventricular myocytes. *Pflugers Arch.* 432:433–438.

Yamaoka, K., and I. Seyama. 1996b. Regulation of Ca channel by intracellular Ca^{2+} and Mg^{2+} in frog ventricular cells. *Pflugers Arch.* 431:305–317.

Zhang, J.F., P.T. Ellinor, R.W. Aldrich, and R.W. Tsien. 1994. Molecular determinants of voltage-dependent inactivation in calcium channels. *Nature.* 372:97–100.

Zuhlke, R.D., G.S. Pitt, K. Deisseroth, R.W. Tsien, and H. Reuter. 1999. Calmodulin supports both inactivation and facilitation of L-type calcium channels. *Nature.* 399:159–162.

Zuhlke, R.D., G.S. Pitt, R.W. Tsien, and H. Reuter. 2000. Ca^{2+}-sensitive inactivation and facilitation of L-type Ca^{2+} channels both depend on specific amino acid residues in a consensus calmodulin-binding motif in the α1C subunit. *J. Biol. Chem.* 275:21121–21129.